Proceedings of the Institute of Acoustics

CRITERIA FOR CHOOSING PROPAGATION MODELS FOR REALISTIC ENVIRONMENTS

M A Ainslie

YARD Ltd, 233 High Holborn, London, WC1V 7DJ.

1. INTRODUCTION

Propagation of sound under water beyond the immediate spherical spreading region (typically at ranges greater than a water depth) can be very sensitive to small variations in sound speed with depth [1] and with the exception of some very special cases [2,3] analytical solutions are not available. For this reason many numerical models have been developed over the past 20 years or so [4] and these have been reviewed by a number of different authors [5-7]. However, these models all make different assumptions and approximations, and it is usually not obvious which, if any, is best suited to a particular problem. One possible approach is to develop diagnostics [8] to check a numerical solution a posteriori and the comparisons thus obtained are very useful in their own right. Nevertheless, it is clearly desirable to choose a suitable model to start with, and no widely applicable method exists for doing so - users rely on the cumulative experience of experts for advice.

One might expect that eventually, one model would emerge as an outright winner and gain a reputation of being the best available. The reason why this has not happened is that the needs of different types of users differ widely, although it is fair to say that the choice usually amounts to a compromise between speed and accuracy. The aim of this paper is to provide guidance on how best to achieve this compromise.

2. VARIOUS CRITERIA

There are, of course, many possible reasons for preferring one model over another: the needs of an operational user at sea will be very different from those of research. Most can be grouped into one of three different categories, referred to here as applicability, validity and practicality.

2.1 Applicability Criteria

This term is related to the correctness of the underlying assumptions of a model, either to do with the acoustic environment or the sonar parameters. For example, are the effects of properties such as shear speed or porosity taken into account? Can the source be assigned a bandwidth or beam pattern? Other effects which spring to mind which may or may not be modelled are, in no particular order, surface roughness and other boundary loss mechanisms, range dependence (2D or 3D), anisotropy, etc.

2.2 Validity Criteria

Even though a model may be applicable in the above sense, it may be that a parameter or effect is treated only approximately. For example the Kirchoff approximation is often used for surface scattering, the effects of shear waves are sometimes treated as perturbations to the fluid solution, the paraxial approximation is used to solve the wave equation in PE (Parabolic Equation) models and so on. The validity of a model then is related to the accuracy of any such approximations.

2.3 Practicality Criteria
Finally, there are practical considerations which may influence the choice of model over and above those of applicability and validity. The user must take into account:

- Availability of the model, implemented on a suitable computer. This covers constraints such as cost, execution time, disk storage, memory size. In addition, finite array sizes chosen by the programmer will inevitably impose limits on the values of some input parameters (most obviously, the frequency).

- Availability of suitable input data. An obvious example is the difficulty in measuring the properties of the sea-bed in deep water. While the most accurate (wave theory) models available require geo-acoustic parameters [9] to describe the sediment and substrate, in practice the ocean bottom is often described by means of a reflection loss table, thus restricting the choice mainly to ray tracing models.

- Robustness of the model, ie. sensitivity to numerical parameters such as mesh size.

- Accuracy of the numerical solution method due to truncation and rounding errors (eg. for solving large matrix problems). Arguably this could be classified under the "Validity" heading but because these problems are, in general, implementation dependent, it is considered here to be a practical problem, not fundamentally associated with limitations of the model itself.

2.4 Chosen Criteria
Any attempt at tackling all or most of the considerations described above is beyond the scope of this paper. Here we concentrate on a more tractable problem - simple enough for all widely available propagation models to be applicable while sufficiently general to be of widespread interest - and compare the accuracy of the models' approximations (validity) by means of the effective angle (Section 3) and their respective computation times (practicality, Section 4). The chosen model problem is that of propagation from a point CW source in a horizontally stratified fluid medium bounded above by a pressure release surface.

3. EFFECTIVE ANGLE

3.1 Background
It is common knowledge that surface/bottom losses often result in steep angle ray paths decaying faster than shallower grazing angles which interact with the boundaries less frequently or not at all. This results in an effective limit to the angle of propagation which tends to reduce with increasing range, referred to from now on as the effective angle θ_e (eg. Weston (Reference 10) - In passing, note also Weston's Figure 1 showing a graph of the number of modes vs number of rays as a function of range, depth and frequency. Without addressing validity, such a graph could form the basis of a criterion for choosing a ray or mode model from a practical point of view).

It is shown in Reference 7 how the validity of many numerical methods can be described in terms of an upper limit to allowed grazing angles Θ, beyond which the approximations made break down. The criterion proposed here is that if Θ exceeds the effective angle θ_e, the model is considered to be valid and is capable of an accurate solution to our model problem. Values of Θ are for PE (Parabolic Equation [11]), NM (Normal Mode [12]) and FF (Fast Field [13]) programs respectively

$\Theta_{PE} \sim 20°$ [14]

$\Theta_{NM} = \cos^{-1}(c/c_m)$

$\Theta_{FF} = \cos^{-1}(c/c_m)$

where c is the sound speed at the source and c_m is the phase speed of the highest wavenumber modelled. In the case of Θ_{NM} it corresponds to the highest order mode (for example in a Pekeris duct, Θ_{NM} would usually be the critical angle). In Fast Field programs c_m is actually an input parameter, thus giving the user complete control over Θ_{FF} in exchange for reduced range capability [7]. Although it is possible to define a value of Θ for ray tracing models in the sense that errors would necessarily be incurred for steeper angles (for example by rays splitting into two on reflection at the sea-bed), it is not done here to avoid giving the incorrect impression that a ray solution would be accurate at smaller angles.

Weston [15] defines an effective angle by means of the equation for intensity I as a function of range r and water depth H:

$$I = \frac{2\theta_c}{rH} \tag{3.1}$$

which he uses to analyse the propagation in the cylindrical spreading (Weston's region B) and mode stripping (C) regimes in range dependent environments. In fact what is meant here by the concept is simply the angle of the steepest ray path which makes a significant contribution to the field (see Reference 7. Eqn (3.1) is consistent with this loose but more general definition in regions B and C.

The most important distinction between this paper and the effective angle curves given by Harrison [7] is the introduction of a short range regime in which the direct path dominates over bottom reflections. The effect is to limit the effective angle to a maximum of $\tan^{-1}(2H/r_{BL})$ where r_{BL} is the transition range to bottom reflection. It will be seen later that the steepest angles (and hence greatest difficulty for the models) occur in deep water and for this reason the effective angle theory is developed for a simple deep water environment with source and receiver close to the surface as illustrated in Figure 1.

3.2 Isovelocity

Initially the ocean is assumed to have a constant sound speed $c_w = c_0$ (Figure 1a) and the effects of refraction in the water are then taken into account separately (Section 3.3). In essence, the intensity can be thought of as the result of adding the contributions from three different components (Figure 1 b-c):

1 = Direct/surface reflected path (DP)
2 = Bottom reflected path (BL)
3 = Bottom refracted path (BR)

Analysis of Figure 1 shows that the angles associated with each component are

$$\theta_{DP} = \tan^{-1}\frac{z_s + z_r}{r} \tag{3.2}$$

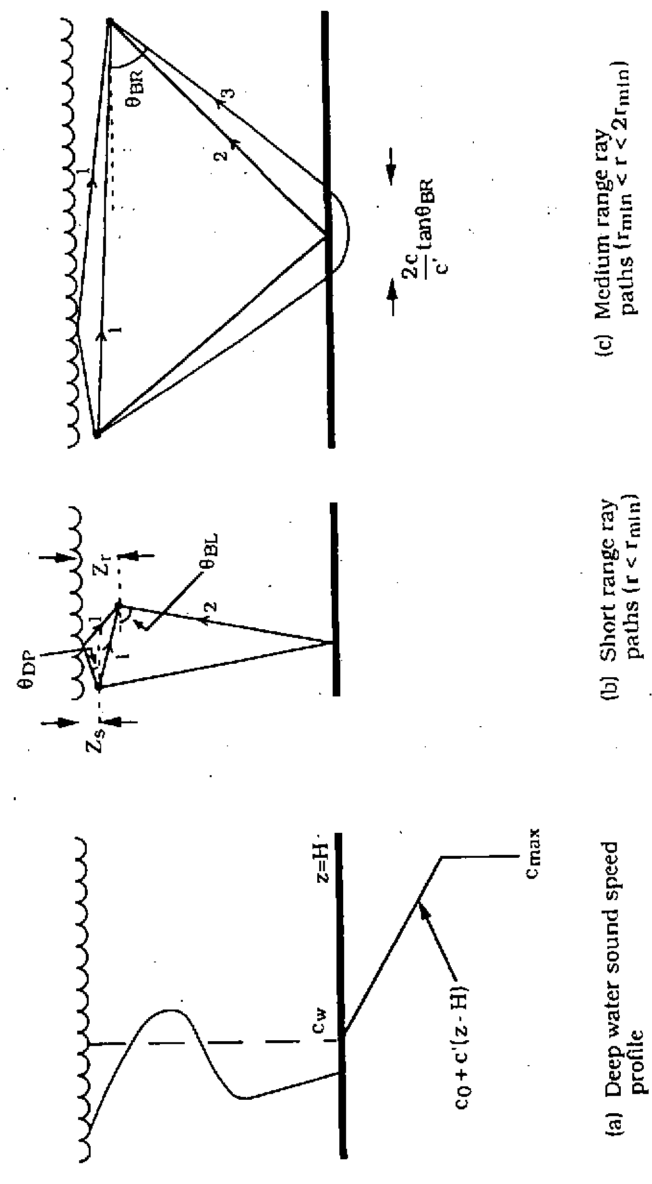

Figure 1 - Deep Water Scenario

CRITERIA FOR CHOOSING PROPAGATION MODELS

$$\theta_{BL} = \tan^{-1}\frac{2H}{r} \tag{3.3}$$

$$\theta_{BR} = \tan^{-1}\left[\frac{c'r}{4c_0}\left(1-\sqrt{1-\frac{16c_0H}{c'r^2}}\right)\right] \qquad r > r_{min} \tag{3.4}$$

where the steeper bottom refracted path [8] has been neglected because it is rarely of practical interest. The value of θ_{BR} is undefined for r less than r_{min} (the range of the first refracted arrival, equal to the caustic range if there is one - see eqn (3.15)).

Multiple reflections/refractions are of course possible but in the case of θ_{BL} may be ignored because they cannot carry much energy compared to the first bottom bounce. This is because having assumed a continuous sound speed across the water-sediment interface, the reflection coefficient

$$R = \left(\frac{\rho-1}{\rho+1}\right)^2 << 1 \tag{3.5}$$

is small for realistic values of the sediment density ρ. For the BR component, at ranges r > $2r_{min}$, we do need to consider multiple returns and it is more convenient to use Weston's definition here, giving

$$\theta_{BR} = \begin{cases} \cos^{-1}\frac{c_0}{c_{max}} & r_{min} < r < r_{15} \\ \left(\frac{\pi H}{4\eta r}\right)^{1/2} & r_{15} < r \end{cases} \tag{3.6}$$

subject to a lower limit of eqn (3.4), where

$$r_{15} = \frac{\pi H}{4\eta}\left[\cos^{-1}\frac{c_0}{c_{max}}\right]^{-2} \tag{3.7}$$

is the transition range from cylindrical spreading to mode stripping and

$$\eta = \frac{4\pi f}{c'}\varepsilon \tag{3.8}$$

Here f is the frequency and ε is the fractional imaginary part of the sediment wavenumber such that

$$k_0 = \frac{2\pi f}{c_0}(1 + i\varepsilon) \tag{3.9}$$

$$\varepsilon = \frac{a}{40\pi\log_{10}e} \tag{3.10}$$

where a is the sediment attenuation coefficient in dB per wavelength. Weston's (Reference 10) loss per unit angle α is related to η by

$$\alpha = (20\log_{10}e)\eta \qquad (3.11)$$

If we can establish which of the three components is dominant for a given geometry, we can use eqns (3.2), (3.3) and (3.6) to construct $\theta_c(r)$. Starting at very short range (Figure 1b), spherical spreading (r^{-2}) ensures that the Direct Path is most important. As range increases into the far field of the surface dipole the DP falls off as r^{-4} and the steep bottom bounce will take over. At still larger range, the BR return will eventually dominate (because R << 1). These simple observations can be summarised on a graph of effective angle vs range as shown in Figure 2. Note that $z_{s,r} << r$, and hence $\theta_{DP} = 0$ have been assumed. The transition ranges r_{BL} and r_{BR} (derived in Appendix 1 by comparing the relative intensifies of the three components) are given by

$$r_{BL} = 2H\max(\beta,\beta^2) \qquad (3.12)$$

$$r_{BR} = \max\left[r_{min}, \frac{4\eta H}{\ln(1/R)}\right] \qquad (3.13)$$

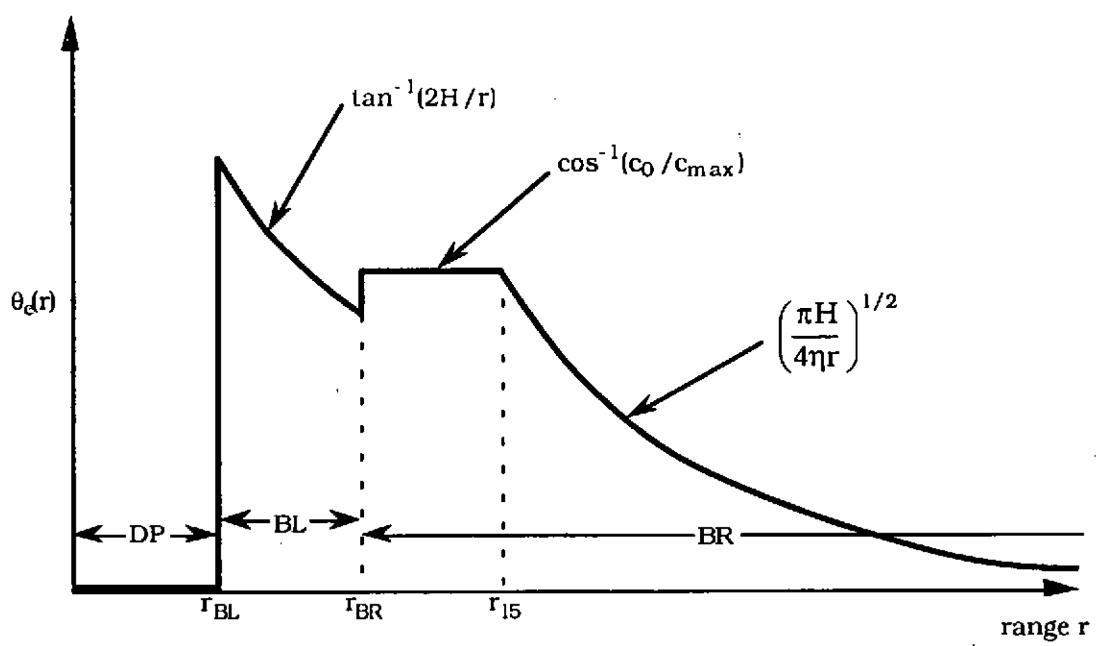

Figure 2 - Effective angle as a function of range in an isovelocity deep water environment for r >> $z_{s,r}$

CRITERIA FOR CHOOSING PROPAGATION MODELS

where

$$\beta = \left[\frac{k z_s z_r}{2HR^{1/2}}\right]^{1/2} \quad (3.14)$$

$$r_{min} = 2H\cot\theta_s + 2\frac{c_0}{c'}\tan\theta_s \quad (3.15)$$

$$\theta_s' = \min\left[\cos^{-1}\frac{c_0}{c_{max}}, \tan^{-1}\left(\frac{Hc'}{c_0}\right)^{1/2}\right] \quad (3.16)$$

In practice, not all parts of the $\theta_e(r)$ curve are necessarily present. For example if $r_{BL} > r_{BR}$ (deep source/receiver) there is no BL dominated region, or if $r_{15} < r_{BR}$ (high frequency) the BR plateau vanishes and there is no cylindrical spreading region.

3.3 Refraction Effects

The relative steepness of the bottom interacting paths means that, in deep water at least, they are basically unaffected by refraction in the water. The DP component on the other hand is approximately horizontal and is very sensitive to refraction.

A negative gradient ($c_w' < 0$) results in a shadow in the direct path at a range

$$r_h = \left|\frac{2c}{c_w'}\right|^{1/2} (z_s^{1/2} + z_r^{1/2}) \quad (3.17)$$

and can be taken into account without difficulty by redefining

$$r_{BL} = \min\left[r_h, 2H\max\left(\beta, \beta^2\right)\right] \quad (3.18)$$

A positive gradient can result in an enhanced DP component depending on the strength of the duct which in turn depends on the duct depth, frequency, source/receiver depths and the gradient c_w' in a complicated way [16]. Because of this complexity, no attempt is made here to compare the duct strength with BL and BR components. Instead we take the worst case and simply assume that $\theta_e(r)$ is unaffected by upward refraction, except where $\theta_e < \theta_{DP}$ would result in which case $\theta_e = \theta_{DP}$ is used. Under these circumstances, θ_{DP} is the maximum angle sustainable in the duct as determined by the velocity contrast

$$\theta_{DP} = \left(\frac{2\Delta c}{c}\right)^{1/2}. \quad (3.19)$$

3.4 Examples

The first example illustrating the use of the effective angle concept is a simple deep water (H = 4000m, $c' = 1s^{-1}$, $\rho = 1.92$, $c_{max} = 2000ms^{-1}$, $a = 0.45$ dB/λ) isovelocity case taken from Reference 8.

CRITERIA FOR CHOOSING PROPAGATION MODELS

Figure 3 shows $\theta_e(r)$ for this environment with z_s = 15m, z_r = 30m for three different frequencies 25Hz, 250Hz, 21/2kHz. Note first of all the very high angles (up to 82°) required at 25Hz, far exceeding the values of Θ_{PE} ~20° and $\Theta_{NM} = \cos^{-1}$ (1500/2000) = 41°, and thus explaining the failure of IFD, PAREQ and SUPERSNAP (Figures 7 - 9 of Reference 8) to reproduce the SAFARI result (Figure 6 of Reference 8 - reproduced here as Figure 4) using a maximum phase speed c_m = 10^5 ms^{-1} (giving Θ_{FF} = 89°).

At 250Hz, θ_{max} (the maximum value of $\theta_e(r)$) is reduced to 67°, still too steep for SUPERSNAP. Increasing the frequency still further to 21/2kHz, we can see from Figure 3 that θ_{max} is reduced to 32° and we can expect NM models to work in principle, though the computational cost may become prohibitive. An additional factor to bear in mind at frequencies above 1kHz or so is that surface losses and volume attenuation, so far ignored, will begin to influence the propagation (see Section 3.6.1).

If the sediment attenuation is reduced, the BR returns will of course be enhanced and a plateau region in $\theta_e(r)$ is clearly visible at 25Hz in Figure 5 (as Figure 3 but a = 0.045 dB/λ). The corresponding SAFARI result, shown in Figure 6, is very similar to Figure 4 except that at ranges greater than r_{min} = 12km the propagation is greatly enhanced, confirming the predominance of bottom refractions in this region.

3.5 Rule of Thumb

It is clear from the above examples that, in deep water, the maximum effective angle θ_{max} is dictated primarily by r_{BL}, the range at which bottom reflected paths exceed the direct path in magnitude. Ignoring the influence of refraction, it follows from eqn (3.12) that if (β < 1), then $\theta_{max} = \cot^{-1}\beta > 45°$, ie. steep enough to ensure some difficulty in modelling. Conversely if $\beta > 1$ (high frequency, shallow water) θ_{max} is likely to be governed by the BR plateau, ie. $\theta_{max} \leq \cos^{-1}(c/c_{max}) = \Theta_{NM}$, guaranteeing the validity of normal mode models at least. The point is that $\beta = 1$ divides two quite different regimes and the magnitude of β provides an excellent indicator of likely problems.

A simple rule of thumb is that in shallow water ($\beta >> 1$) steep angles are unlikely to be a problem and any of the above models may be used, whereas in deep water ($\beta \lesssim 1$) steep angles are almost inevitable and careful consideration must be given to effective angles before a model is selected. Note that this distinction between deep and shallow water is quite different from the conventional association with plentiful modes and high frequency. On the contrary, it is clear from eqn (3.14) that the higher the frequency, the larger β becomes and the shallower the water appears.

Possible values of β in realistic situations (frequency 10Hz to 10kHz, water depth 40m to 4km, source/receiver depth 10m to 300m) vary between 10^{-2} and 10^{+2}. For the environment considered in Section 3.4, β varies between 0.1 (at 25Hz) and 1.4 (2.5kHz).

3.6 Miscellaneous Effects

The effective angle theory in Section 3 initially assumed an isovelocity, deep water environment and a low frequency source, although the isovelocity constraint was removed in Section 3.3. The purpose of this Section is to examine the significance of the other two constraints and to show how they too can be removed.

3.6.1 High Frequency. When the frequency exceeds 1kHz or so, the assumption that surface and volume losses can be ignored no longer holds. For example poor reflection means that the surface dipole is no longer symmetrical, so that perfect cancellation is no longer possible and

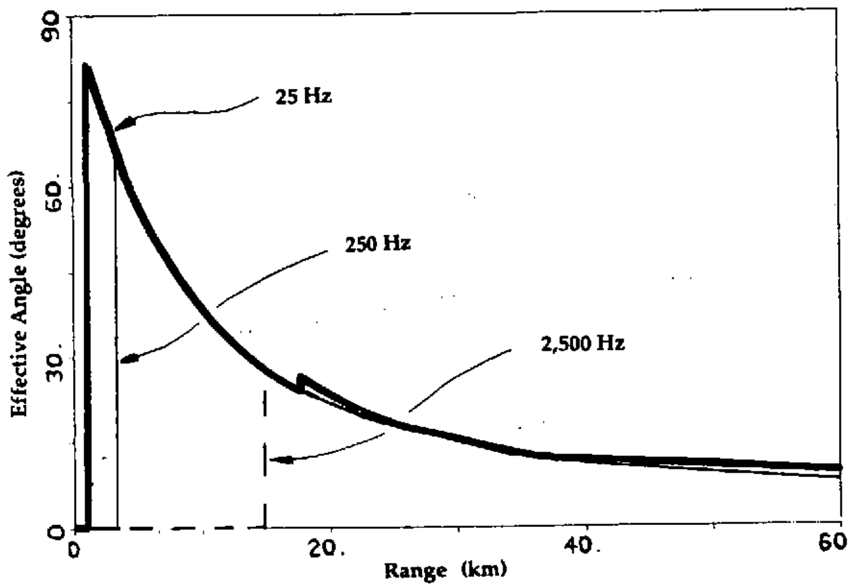

Figure 3 - Effective Angle vs Range
(a = 0.45dB/λ)

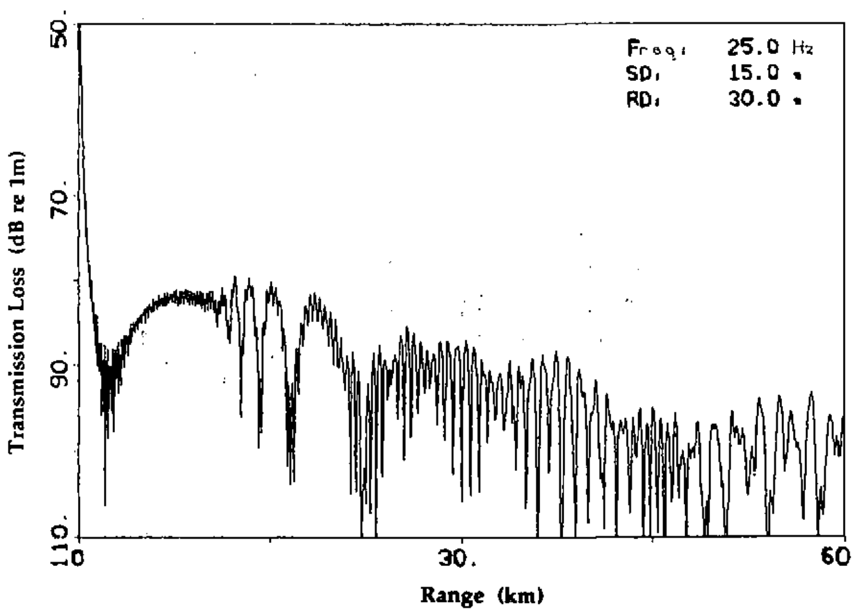

Figure 4 - Tranmission Loss vs Range
(a = 0.45dB/λ)

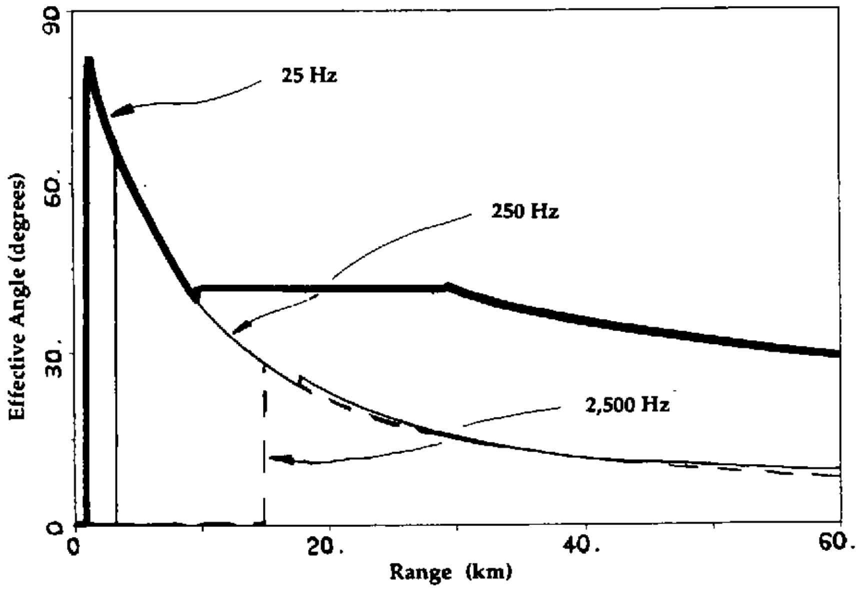

Figure 5 - Effective Angle vs Range
(a = 0.045dB/λ)

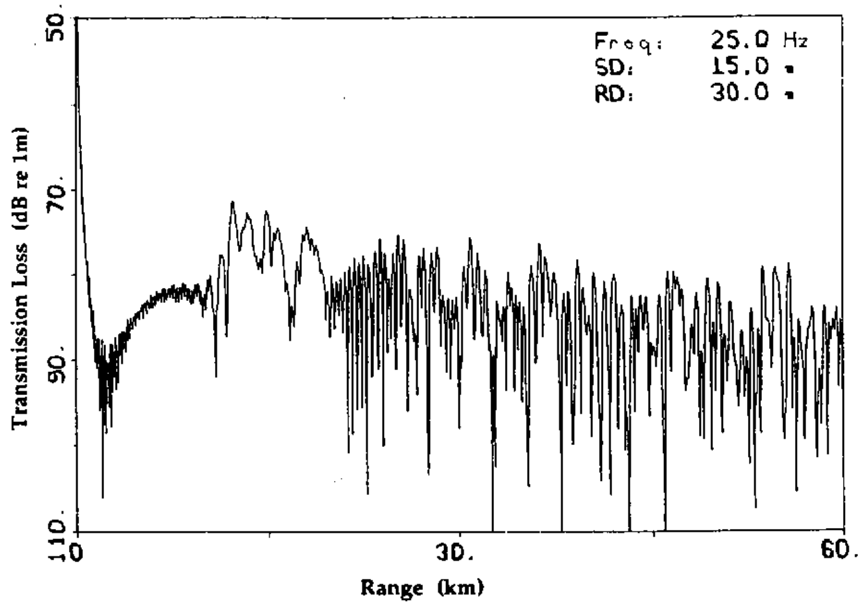

Figure 6 - Tranmission Loss vs Range
(a = 0.045dB/λ)

the DP is characterised by r^{-2} instead of r^{-4} at long range. As far as volume attenuation is concerned, the longer path length of the BL component compared to DP means that it will suffer greater attenuation. Both effects result in a stronger DP (relative to BL) and hence larger r_{BL} and smaller effective angles. The existing theory can therefore be used unmodified to obtain an upper bound on the true effective angle, in a similar way as for upward refraction ($c_w' > 0$).

3.6.2 Shallow Water. In the present context the "deep water" assumption covers a multitude of sins, and these are considered in turn.

Firstly, throughout this paper it has been implicitly assumed that the ray arguments of Section 3.2 are applicable, for which we required $kH >> 1$. In fact this inequality is satisfied automatically at all frequencies above 25Hz so long as the water depth is 100m or more.

Second, the assumed geometry required $z_{s,r} << H$. Removing this limitation simply makes the equations of Section 3 more complicated without adding any insight and without affecting any of the conclusions.

Finally, the sea-bed characteristics chosen are typical of deep water but not shallow water (continental shelf) sediments, which are frequently modelled with an isovelocity fast bottom ($c_0 > c_w$, $c' = 0$). This Pekeris duct problem can be catered for by replacing eqns (3.8) and (3.15) with

$$\eta = 2\rho \sec\theta_c \cot^3\theta_c \varepsilon$$

$$r_{min} = 2H\cot\theta_c$$

where

$$\theta_c = \cos^{-1}(c_w / c_0)$$

is the critical angle, and the role of the bottom refracted component is taken by totally internally reflected paths. It is interesting to note that although this situation is equivalent to putting $c_0 = c_w$, $c' \to \infty$, $\theta_c = \cos^{-1}(c_0/c_{max})$, substituting these limits into Section 3.2 (and in particular eqn (3.8)) leads to the erroneous conclusion that $\eta \to 0$. This discrepancy arises because the use of the Rayleigh reflection coefficient requires the gradients on either side of the boundary to be small.

4. COMPUTATION TIME

4.1 Total Solution Time

The total time taken to obtain a transmission loss solution once a decision has been made to use a particular model on grounds of validity is made up of several steps, not all of which need to be repeated for subsequent runs, as follows:

- The time required for obtaining the model, possibly from abroad, and implementing it.
- Obtaining the necessary input data and creating formatted input files.
- Computation time.
- Analysis of output, possibly including further computer runs to check for convergence.

CRITERIA FOR CHOOSING PROPAGATION MODELS

Although any or all of these may be important, the "speed" of a model is usually a reference to the computation time T. Comparison of T with some acceptable upper limit (which would depend on the circumstances) can be a useful criterion because it is the one ingredient which is always present. Compared with the other steps it is also relatively easy to quantify. Nevertheless the potential user should bear in mind that analysis time (checking the result) is frequently the biggest single item once a program is fully implemented. In practice this means that robustness should be high on one's list of priorities, irrespective of application.

Estimates of computer time used by several common models for a point source in a range independent environment are as follows:

4.2 Parabolic Equation CPU Time
For a Gaussian start-up field CPU Time [14], the CPU time taken for PE models for a point source in a range independent environment to compute the sound field to a maximum range r is approximately

$$T_{PE} \simeq A_{PE} \frac{H_{PE}}{\delta H} \frac{r}{\delta r} \qquad (4.1)$$

where H_{PE} is the total computation depth which must exceed the water depth by an amount depending on the extent of acoustic penetration of the sediment. The step sizes δH, δr are typically around $\lambda/4$ and hence

$$T_{PE} \sim 16 A_{PE} \frac{H_{PE} r}{\lambda^2}, \qquad (4.2)$$

although substantially smaller or larger values may sometimes be appropriate, especially in range-dependent environments. In principle, it is possible to vary δH and δr as the solution marches in range choosing small steps only when it is necessary to do so [17].

Some implementations allow a normal mode start-up field which will involve an overhead similar in magnitude to the value of T_{NM} (eqn (4.3)).

It is worth bearing in mind that PE models calculate the entire 2D field automatically so that there is no overhead for multiple receiver depths.

4.3 Normal Mode CPU Time
If only one receiver depth is calculated, the CPU requirement for a normal mode program tends to be dominated by the numerical calculation of eigenfunctions and corresponding eigenvalues. The solution time varies greatly according to the method - for SUPERSNAP [18] which uses a matrix method devised by Porter & Reiss (Reference 19), it is

$$T_{NM} \simeq A_{NM} \left(\frac{H}{\delta H}\right)^{1/2} N_{modes} \qquad (4.3)$$

where δH is the eigenfunction sampling distance used in the matrix solution, and is typically around $\lambda/50$. Assuming that N_{modes} (the number of modes) is approximately H/λ, this then gives

$$T_{NM} \sim 7A_{NM}\left(\frac{H}{\lambda}\right)^{3/2} \quad (4.4)$$

4.4 Fast Field CPU Time
As with normal mode programs, computation time for the fast field method can vary greatly according to the implementation. For SAFARI [20] it is given by

$$T_{FF} \simeq A_{FF} N_L N_{FFT} \quad (4.5)$$

where N_L is the number of layers used (the number of points in the sound speed profile) and N_{FFT} is the number of points used to perform the discrete Fourier Transform, which for a wide angle run is just r/λ, ie

$$T_{FF} \sim N_L A_{FF} \frac{r}{\lambda} \quad (4.6)$$

This linear dependence on frequency means that at high frequency, SAFARI is more economical than either normal mode ($T_{NM} \sim f^{3/2}$) or parabolic equation ($T_{PE} \sim f^2$) programs. In particular, (comparing eqn (4.2) with (4.6)) T_{PE} will exceed T_{FF} at all frequencies above

$$f = \frac{N_L}{16}\frac{A_{FF}}{A_{PE}}\frac{c}{H_{PE}}$$

which in deep water (eg. H_{PE} = 5,000m, N_L = 20) can be as low as 20Hz.

4.5 Ray Trace CPU Time
The computation time required by the ray tracing program GRASS [21] is given by

$$T_{RT} \simeq A_{RT} N_{rays} \frac{r}{\delta r} \quad (4.7)$$

It is difficult to make general statements about how the range step δr (the horizontal distance between adjacent receiver positions) and the number of rays N_{rays} should vary with frequency and water depth. Typical values for coherent calculations in deep water at 1kHz are N_{rays} ~5,000 and δr ~50m, although substantial savings in both are possible for incoherent intensity calculations.

4.6 Constants of Proportionality
The absolute values of the "constants" A_{PE}, A_{NM} etc can of course vary by orders of magnitude from one computer to another although hopefully their relative values will stay roughly constant. Order of magnitude values based on the author's own experience for typical problems for a VAX 11/750 are

A_{PE} ~ 10^{-3}s

A_{NM} ~ 10^{0}s

A_{FF} ~ 10^{-1}s

A_{RT} ~ 10^{-3}s

CRITERIA FOR CHOOSING PROPAGATION MODELS

Nevertheless, exceptions are common. For example:

- The value of A_{FF} is reduced by an order of magnitude if only isovelocity layers are used in SAFARI.
- The expressions for T_{NM}, T_{FF} and T_{RT} will require modification if a large number of receiver depths are required (eg. for a contour plot).

5. SUMMARY AND CONCLUSIONS

Criteria are presented for making an objective selection of a propagation model, based on a compromise between the accuracy of the models' approximations involving propagation angle, and computational speed. The effective angle theory is developed initially for low frequency, deep water propagation (Section 3) although in Section 3.6 it is shown how it can be applied to high frequency and/or shallow water. A useful rule of thumb is given in Section 3.5 for deciding whether or not angles are an issue at all. The CPU time requirement for a number of different types of model are discussed in Section 4.

The criteria could be used as part of a logic tree which also took into account the wider questions of applicability and practicality described in Section 2. The procedure could even be automated to provide expert advice on which model to use with reasoning, along with recommended values of numerical input parameters. Eventually, one can envisage a situation where a computer system selects and runs a computer model without the user being involved beyond giving acoustic input parameters and the relevant practical constraints.

ACKNOWLEDGEMENT

This work has been carried out with the support of the Procurement Executive, Ministry of Defence.

APPENDIX - CALCULATION OF TRANSITION RANGES r_{BL} AND r_{BR}

Direct Path to Bottom Reflection

At low frequency in isovelocity water, the interference between the direct path and a single surface reflection results in the well known Lloyd's Mirror formula

$$I_{DP} = \frac{4}{r^2}\sin^2\frac{kz_s z_r}{r} \qquad (A.1)$$

and the bottom reflected intensity is [8]

$$I_{BL} = 16\frac{\cos^2\theta_{BL}}{r^2}\sin^2(kz_s\sin\theta_{BL})\sin^2(kz_r\sin\theta_{BL})R \qquad (A.2)$$

Assuming $R << 1$, it is clear that I_{DP} will always exceed I_{BL} on average, until r exceeds kz_sz_r and the DP begins to fall off as r^{-4}. The range at which the transition takes place (r_{BL}) can therefore be found by replacing the $\sin^2$ functions by either their mean value 1/2 (in the case of BL) or argument kz_sz_r/r (DP), ie.

CRITERIA FOR CHOOSING PROPAGATION MODELS

$$4\left(\frac{kz_s z_r}{r_{BL}^2}\right)^2 = \frac{4\ R}{r_{BL}^2 + 4H^2} \qquad \text{(A.3)}$$

a quadratic in $r_{BL}{}^2$ whose solution is

$$r_{BL}^2 = (2H\beta^2)^2\left[\tfrac{1}{2} + \left(\tfrac{1}{4} + \beta^{-4}\right)^{1/2}\right]. \qquad \text{(A.4)}$$

Noting that the factor in square brackets is equal to 1 for large β and β^{-2} for small β, we can write, very crudely

$$r_{BL} \doteq 2H\ \max(\beta, \beta^2) \qquad \text{(A.5)}$$

Bottom Reflection to Bottom Refraction

At sufficiently long range (such that $\theta_{BR} << c'H/c$), the expression for bottom refracted intensity (see Reference 8) is very similar to eqn (A.2)

$$I_{BR} = 16\frac{\cos^2\theta_{BR}}{r^2}\sin^2(kz_s\sin\theta_{BR})\sin^2(kz_r\sin\theta_{BR})\,R' \qquad \text{(A.6)}$$

where R' is the effective reflection coefficient for the refracted path caused by volume attenuation in the sediment, and for a sediment path length s, is given by exp $[-2k\varepsilon s]$.

At long range, the small grazing angles result in correspondingly small sediment path lengths and eventually R' tends to 1. When this happens the BR returns will dominate the sound field, with the cross-over (BL to BR) occurring when R and R' are approximately equal, ie.

$$\ln(1/R) = 2k\varepsilon s \qquad \text{(A.7)}$$

where

$$s \doteq \frac{2c}{c'}\theta_{BR}\ . \qquad \text{(A.8)}$$

Replacing θ_{BR} with its long range approximation $2H/r_{BR}$ in eqn (A.7) it follows straight away that

$$r_{BR} = \frac{4H\eta}{\ln(1/R)}\ . \qquad \text{(A.9)}$$

This then is the range for the BL-BR transition, subject to a lower limit dictated by the shadow in the refracted path. The position of the shadow is given either by the caustic range if there is one

CRITERIA FOR CHOOSING PROPAGATION MODELS

$$r_c = 4\left(\frac{Hc}{c'}\right)^{1/2}$$

or if not, by the ray which just grazes the bottom of the sediment. In either case, the shadow boundary is at r_{min} as defined by eqn (3.15).

REFERENCES

[1] H WEINBERG, Application of ray theory to acoustic propagation in horizontally stratified oceans, J. Acoust. Soc. Am. 58(1), 97-109 (1975).

[2] N C NICHOLAS & H ÜBERALL, Normal-mode propagation calculations for a parabolic velocity profile, J. Acoust. Soc. Am. 48(3), 745-752 (1970).

[3] M J BUCKINGHAM, Theory of acoustic propagation with an inverse-square sound speed profile, submitted to J. Fluid Mech.

[4] P C ETTER, A survey of underwater acoustic models and environmental-acoustic data banks, ASWSPO Report ASWR-84-001, April 1984.

[5] F R DINAPOLI & R L DEAVENPORT, Numerical models of underwater acoustic propagation, in Ocean Acoustics, ed J A DeSanto, Pub Springer-Verlag 1979.

[6] F B JENSEN & W A KUPERMAN, Deterministic propagation modelling II: Numerical results, in Underwater Acoustics and Signal Processing, ed L Bjorno, Pub D Reidel 1980.

[7] C H HARRISON, Ocean propagation models, Applied Acoustics 27, 163-201 (1989).

[8] M A AINSLIE & C H HARRISON, Diagnostic tools for the ocean acoustic modeller, Proc. 2nd IMACS Symposium on Computational Acoustics, Princeton, March 1989.

[9] E L HAMILTON, Geoacoustic modeling of the sea floor, J. Acoust. Soc. Am. 68(5), 1313-1340 (1980).

[10] D E WESTON, Intensity-range relations in oceanographic acoustics, J. Sound Vib. 18, 271-287 (1971)

[11] F D TAPPERT, The parabolic approximation method, in Wave Propagation and Underwater Acoustics, ed J B Keller & J S Papadakis, Springer-Verlag, Berlin, 1977.

[12] J F MILLER & F INGENITO, Normal mode FORTRAN programs for calculating sound propagation in the ocean, NRL Memo Report No. 3071, 1975.

[13] F R DINAPOLI & R L DEAVENPORT, Theoretical and numerical Green's function field solution in a plane multilayered medium, J. Acoust. Soc. Am. 67(1), 92-105 (1980).

[14] D LEE & S T MCDANIEL, Comput. Math. Applic. 14(5), 305-423 (1987).

[15] D E WESTON, Propagation in water with uniform sound velocity but variable-depth lossy bottom, J. Sound Vib. 47 (4), 473-483 (1976).

[16] D E WESTON, Acoustic flux formulas for range-dependent ocean ducts, J. Acoust. Soc. Am. 68(1), 269-281 (1980).

[17] J S ROBERTSON, D C ARNEY, M J JACOBSON & W L SIEGMANN, An efficient enhancement of finite-difference implementations for solving parabolic equations, J. Acoust. Soc. Am. 86(1), 252-260 (1989).

[18] F B JENSEN & M C FERLA, SNAP: the SACLANTCEN normal mode acoustic propagation model, SACLANT Report SM-121, 1979.

[19] M B PORTER & A REISS, A numerical method for bottom interacting ocean acoustic normal modes, J. Acoust. Soc. Am. 77(5), 1985.

[20] H SCHMIDT, Seismo-Acoustic Fast field Algorithm for Range Independent environments - User's Guide, SACLANT Report SR-113, September 1988.

[21] J J CORNYN, GRASS: A digital-computer ray-tracing and transmission loss-prediction system, Volume 2 - User's Manual, NRL Report 7642, December 1973.